Competing single-particle and collective structures in ^{86}Nb

S. L. Tabor, J. Döring,* G. D. Johns,† R. A. Kaye, and G. N. Sylvan
Department of Physics, Florida State University, Tallahassee, Florida 32306

C. J. Gross
ORISE, Oak Ridge Associated Universities, Oak Ridge, Tennessee 37831
and Physics Division, Oak Ridge National Laboratory, Oak Ridge, Tennessee 37831

Y. A. Akovali, C. Baktash, and D. W. Stracener
Physics Division, Oak Ridge National Laboratory, Oak Ridge, Tennessee 37831

P. F. Hua, M. Korolija, D. R. LaFosse, and D. G. Sarantites
Chemistry Department, Washington University, St. Louis, Missouri 63130

F. E. Durham
Department of Physics, Tulane University, New Orleans, Louisiana 70118

I. Y. Lee, A. O. Macchiavelli, and W. Rathbun
Nuclear Science Division, Lawrence Berkeley National Laboratory, Berkeley, California 94720

A. Vander Molen
National Superconducting Cyclotron Laboratory, Michigan State University, East Lansing, Michigan 48824
(Received 25 November 1996)

The high-spin structure of odd-odd ^{86}Nb was studied with the early implementation of GAMMASPHERE using 36 Compton-suppressed Ge detectors and the MICROBALL, a 95-element full-sphere charged-particle detector array. High-spin states were populated using the ^{58}Ni(^{32}S,3pn) reaction at 135 MeV with beams from the 88-Inch Cyclotron at Lawrence Berkeley National Laboratory. A number of bands were observed up to spins as high as (31^-). The yrast positive-parity band shares many characteristics with the $\pi g_{9/2} \otimes \nu g_{9/2}$ bands in other odd-odd f-p-g shell nuclei. These similarities include the behavior of the moments of inertia, the magnitude and phase of the signature splitting and its phase reversal near the 10^+ state, and the strong alternations in the $B(M1)/B(E2)$ strengths. The moments of inertia in the lowest pair of negative-parity bands start out with a sharp upbend and then gradually fall back to the rigid-body value. New positive- and negative-parity bands appear in the quasiparticle alignment region and eventually become yrast. Some additional positive-parity states around spin $17\hbar$ are candidates for fully or nearly fully aligned shell-model-like configurations. [S0556-2813(97)04607-4]

PACS number(s): 23.20.En, 23.20.Lv, 25.70.Gh, 27.50.+e

I. INTRODUCTION

Nuclei in the $A \approx 80$ region of deformation where both protons and neutrons fill the same f-p-g shell show strong collective properties with ground-state deformations β_2 exceeding 0.4 in some cases, yet are very sensitive to the polarizing effects of individual particles. They provide an excellent laboratory for studying the interplay between single-particle and collective excitations. The roughly equal proton and neutron numbers also mean that proton and neutron quasiparticle alignments can compete on a nearly equal basis.

Odd-odd nuclei in this region have not been investigated as well until recently because of the greater experimental and theoretical challenges they present. However, several studies in the last few years have shown the existence of rotational bands in odd-odd nuclei which are at least as regular as those in the neighboring nuclei [1–11]. In particular a strong similarity has been seen among the yrast positive-parity bands [12]. They appear to be based on the configuration $\pi g_{9/2} \otimes \nu g_{9/2}$ which provides the maximum intrinsic spin available from two quasiparticles (qp's) in the f-p-g shell: $9\hbar$. Changes that occur in the signature splitting and moments of inertia around spin $9\hbar$ have been interpreted [6,8,13] as a transition from realignment of the intrinsic angular momentum to collective rotation. Regular negative-parity bands have also been observed, but their systematics are less clear.

The regular band structures have mostly been observed in more deformed nuclei with neutron and proton numbers not far from midshell. The behavior of transitional odd-odd nuclei with particle numbers approaching shell closure remains an open question. The odd-odd nucleus ^{86}Nb, only five

*Present address: Department of Physics, University of Notre Dame, Notre Dame, IN 46556.
†Present address: Los Alamos National Laboratory, Los Alamos, NM 87545.

neutrons away from the shell closure at $N=50$, provides an opportunity to investigate such a transitional case. Lighter nuclei closer to midshell generally exhibit rotational bands while heavier nuclei with $N \geqslant 47$ have been successfully described with shell-model calculations [14–16]. Therefore strong competition between single-particle and collective behavior might be expected in ^{86}Nb.

Only one study [17] has been reported on the high-spin structure of ^{86}Nb from an in-beam experiment. This work established 18 new states in two separate decay sequences, although the spins of the states and the relative positions of the two sequences could not be determined. More experimental work was clearly needed before the structure of ^{86}Nb could be placed in the context of other odd-odd nuclei. In addition to the in-beam work, several studies of the β^+/(electron capture) (EC) decay of ^{86}Nb to states in ^{86}Zr [18–21] provide information on the parent state in ^{86}Nb, and one investigation [21] on the β^+/EC decay of ^{86}Mo to states in ^{86}Nb establishes four low-spin states in the daughter nucleus.

The present investigation was begun to provide a more comprehensive picture of the high-spin structure of ^{86}Nb using the resolving power of the early implementation of GAMMASPHERE with the reaction channel selectivity of the MICROBALL to explore the competing roles of single-particle and collective modes in this transitional odd-odd nucleus.

II. EXPERIMENTAL PROCEDURE

High-spin states in ^{86}Nb were populated using the ^{58}Ni(^{32}S,3pn) reaction at 135 MeV with beams from the 88-Inch Cyclotron at Lawrence Berkeley National Laboratory. The target was a ^{58}Ni foil enriched to 99.7% in ^{58}Ni with an effective thickness of 245 μg/cm^2. Gamma rays from the reaction were detected with the early implementation phase of GAMMASPHERE [22] consisting of 36 Compton-suppressed HPGe detectors. The evaporated charged particles were detected and identified with the MICROBALL [23], an array of 95 CsI(Tl) scintillators covering 98% of the full sphere around the target with a proton detection efficiency of 84%.

A total of 4.2×10^8 raw events with three or more γ rays in coincidence were collected. Events with exactly three protons and no α particles were sorted into both a triangular and a square γ-γ matrix for analysis. Pairwise coincidences were also sorted into one of two additional triangular matrices if the third member of a γ triple were any of about six low-lying transitions in each of the two major decay sequences. The triangular matrices [24] which are symmetric in all the detectors were used in constructing the level scheme and determining the relative intensities. Gamma rays from any of the six detectors located at 90° relative to the beam were sorted onto one axis of the square array, while those from any of the 30 detectors at angles of 17.275° – 37.38° and 142.62° – 162.725° were sorted onto the other axis to allow the determination of directional correlation of oriented nuclei (DCO) ratios. For most lines, the DCO ratios were determined from several nearby $E2$ gates and averaged. The DCO ratios used here were calculated according to

$$R_{\mathrm{DCO}}(\gamma_1,\gamma_2)=\frac{I(\gamma_1 \text{ at } 17^\circ \text{ to } 38^\circ \text{ or } 142^\circ \text{ to } 163^\circ \text{ gated by } \gamma_2 \text{ at } 90^\circ)}{I(\gamma_1 \text{ at } 90^\circ \text{ gated by } \gamma_2 \text{ at } 17^\circ \text{ to } 38^\circ \text{ or } 142^\circ \text{ to } 163^\circ)}. \quad (1)$$

The γ detectors were calibrated by least-squares fitting the energies of lines in ^{56}Co, ^{88}Y, and ^{152}Eu to a third-order polynomial (cubic) function of the channel numbers of the centroids of the corresponding peaks. A four-parameter fit was made to the relative efficiencies of the detectors using the lines from ^{152}Eu. The resulting γ-ray energies, intensities, and DCO ratios are listed in Tables I and II for all the transitions placed in the ^{86}Nb level scheme. The intensities listed represent averages over all the angles of observation without any further adjustments for angular correlation effects.

Two follow-up experiments [25] were performed at Florida State University to resolve questions concerning the low-lying level structure of ^{86}Nb. Both experiments used the same reaction as was used in the primary experiment, ^{58}Ni(^{32}S,3pn), with 135 MeV ^{32}S beams from the FSU Superconducting Accelerator Laboratory. First a search was made for low-energy γ transitions down to 12 keV using a low-energy photon spectrometer (LEPS) both alone and in delayed coincidence with the FSU array of five Compton-suppressed Ge detectors. The second experiment was a remeasurement of the β decay of ^{86}Nb using a pulsed beam and the FSU array.

III. RESULTS

The level scheme established in the present work is shown in Fig. 1. The numbers placed above each major decay sequence are intended to facilitate the discussion and do not represent any theoretical interpretation. This level scheme generally confirms the previous work [17], and the presence of the lines in the $3p$-0α particle-gated matrix along with known lines from ^{87}Nb confirms the assignment to ^{86}Nb. Several connecting transitions fix the relative positions of the two strongest decay sequences. The question of the position and spin of the lowest state will be discussed below.

A. Ground state

The identification of the ground state is nontrivial in odd-odd nuclei in this region because states of substantially dif-

TABLE I. Energies, relative intensities, and DCO ratios of transitions among the positive-parity states in ^{86}Nb. The relative intensities are normalized to the 859.8 keV line.

E_x (keV)	I_i^π	I_f^π	E_γ (keV)	I_γ	$R_{\rm DCO}$
26.4	7	6^+	(26.4)		
274.5	8^+	7	248.1(3)	49.6(15)	0.59(3)
		6^+	274.5(3)	63.5(15)	0.82(4)
724.8	9^+	8^+	450.3(3)	20.3(12)	0.48(5)
1134.3	10^+	9^+	409.4(3)	5.5(7)	0.45(5)
		8^+	859.8(4)	100	0.91(8)
1601.3	11^+	10^+	466.9(3)	27.7(12)	0.43(4)
		9^+	876.5(4)	15.6(10)	0.95(8)
2211.7	12^+	11^+	610.2(4)	9.3(11)	
		10^+	1077.6(6)	69.0(20)	0.94(8)
2684.2	13^+	12^+	472.4(3)	13.5(18)	0.42(4)
		11^+	1083.1(5)	26.6(20)	0.97(9)
3468.3	14^+	13^+	784.5(5)	7.0(19)	
		12^+	1256.4(6)	42.3(25)	0.97(9)
3902.5	15^+	14^+	434.0(5)	5.3(12)	0.47(10)
		13^+	1218.4(5)	25.4(14)	0.98(7)
3987.6	15^+	14^+	519.4(4)	10.7(13)	0.48(9)
		13^+	1303.4(4)	31.8(18)	1.00(7)
4841.3	16^+	14^+	1373.0(10)	10(4)	1.03(8) [a]
5027.3	(16^+)	15^+	1124.8(8)	5.3(15)	
5274.2	17^+	16^+	434(1)	3(1)	
		15^+	1286.8(6)	8.6(12)	0.98(9)
		15^+	1371.4(10)	18(6)	1.03(8) [a]
5308.1	17^+	16^+	467.2(7)	9.5(16)	
		15^+	1320.3(7)	26.4(20)	0.97(9)
5533.1	(17^+)	17^+	225.1(4)	2.0(7)	
		17^+	258.8(4)	2.6(8)	
		(16^+)	505.1(8)	4.8(10)	
6362.1	(18^+)	16^+	1520.8(15)	6.3(10)	
6645.2	19^+	(17^+)	1113(2)	3.1(8)	
		17^+	1337.1(5)	20.5(20)	1.00(11)
		17^+	1370.9(10)	8(3)	1.03(8) [a]
6722.5	19^+	18^+	360.6(4)	1.3(3)	
		17^+	1414(2)	4.7(12)	
		17^+	1448.1(10)	10.9(15)	
6957	(19^+)	(17^+)	1424(2)	8(3)	
		17^+	1649(3)	12(3)	
7666	(20^+)	(19^+)	707.4(9)	1.2(4)	
		19^+	1020.6(12)	6.1(18)	0.50(14)
7906.6	21^+	(20^+)	240.9(8)	3.3(9)	0.52(12)
		19^+	1261.4(14)	14.5(20)	0.97(9)
7966.1	(20^+)	(18^+)	1604.0(15)	5.6(12)	
8270.5	(21^+)	19^+	1548.0(15)	11.5(18)	
8602	(21^+)	(19^+)	1645(3)	6(2)	
9382.1	23^+	21^+	1475.5(14)	10.0(20)	0.98(15)
9774	(22^+)	(20^+)	1808(2)	6.5(20)	
10052.8	(23^+)	(21^+)	1782.3(17)	5.7(18)	
10429	(23^+)	(21^+)	1827(3)	4(2)	
11283	(25^+)	23^+	1901(2)	6.0(20)	
12014	(25^+)	(23^+)	1961(3)	3.7(15)	
(12407)	(25^+)	(23^+)	(1978)		
13509	(27^+)	(25^+)	2226(3)	2.0(8)	
13568	(27^+)	(25^+)	2285(3)	1.6(7)	

[a]Combined DCO ratio of the triplet.

ferent spin often lie close to the ground state and β decay independently. Several radioactivity studies [18–20] have established the β^+/EC decay pattern from a state in ^{86}Nb with a half-life of 88(1) s. Since ^{86}Nb was populated in those studies with heavy-ion fusion-evaporation reactions similar to the present one, this 88 s state most likely corresponds to the lowest one in Fig. 1.

A recent measurement [21] of the β^+/EC decay of ^{86}Mo revealed a γ-decay sequence among four new low-spin states in ^{86}Nb ($I^\pi = 0^+ - 2^+$) which does not involve any of the γ rays shown in Fig. 1. This confirms the expected coexistence of low-lying low-spin and high-spin states built on different quasiparticle configurations. The lack of any observed γ transitions between the two sets of levels leaves unanswered the question of which lies lower and forms the ground state.

In nearby odd-odd ^{82}Y [6] γ decays between the low- and high-spin states show that the 4^+ state lies 401 keV above the 1^+ ground state. A low-lying 6^+ state [10] and 1^+ state [26] are known in ^{84}Y, and recent work [27] shows that the 1^+ state lies just above the 6^+ one. In the isobar ^{86}Y [28,29] the 8^+ state lies 218 keV above the 4^- ground state. Based on β end-point energies [30] the (4^-) level lies 40 keV above the (8^+) ground state in the isotope ^{88}Nb, but the uncertainties do not preclude the opposite ordering. Again, the 4^- level in ^{90}Nb lies 125 keV above the 8^+ ground state [31].

Thus there is ample systematic evidence among the nearby odd-odd nuclei that low-spin and high-spin states coexist at low excitation energies. However, the relative ordering varies and no definite conclusion can be drawn about whether the 6^+ state is the ground state of ^{86}Nb. To simplify the discussion in this paper, we will use the term ''ground state'' for the lowest level in Fig. 1.

The spin and parity of the ^{86}Nb ground state (lowest level in Fig. 1) are restricted to 5^+, 6^+, or 7^+ by the observation [20] of an allowed ($\log ft = 5.76$) β decay to the known 6^+ state in ^{86}Zr. A spin parity of 5^+ was suggested [20] for the ^{86}Nb ground state because of the 10.1% β-decay branch to the 4^+ state in ^{86}Zr ($\log ft = 6.47$). However, the authors were concerned that the large $Q_{\rm EC}$ of 8.15 MeV would permit β branches to even higher-lying states which they could not detect due to the decrease in γ detection efficiency with increasing γ energy. Such undetected β branches would then decay to the lower-lying states in ^{86}Zr by unobserved γ rays and lead to an overestimate of the direct β feeding of the lower levels.

A better knowledge of the systematics of odd-odd nuclear structure in this region, which has been acquired since that β-decay work, clearly shows that the spin parity of the ground state of ^{86}Nb is 6^+. All of the lowest ''high-spin'' states in the neighboring odd-odd nuclei have even spin (6^+ or 8^+) as listed above. It will be shown in the following discussion that the yrast band built on the ground state has all the characteristics [12] of the $\pi g_{9/2} \otimes \nu g_{9/2}$ bands in other nuclei if it starts with a state of spin parity 6^+ and not 5^+ or 7^+.

To resolve the discrepancy between the spin assignments of 5^+ suggested [20] from β decay and 6^+ from well-established systematics, the two follow-up experiments de-

TABLE II. Energies, relative intensities, and DCO ratios of transitions among the negative-parity states in ^{86}Nb. The relative intensities are normalized to the 859.8 keV line in the positive-parity band.

E_x (keV)	I_i^π	I_f^π	E_γ (keV)	I_γ	$R_{\rm DCO}$	E_x (keV)	I_i^π	I_f^π	E_γ (keV)	I_γ	$R_{\rm DCO}$
494.2	6^-	6^+	494.2(3)	80.8(15)	0.92(6)			14^-	1089.9(6)	34.9(30)	0.98(9)
887.5	7^-	6^-	393.3(3)	36.0(14)	0.42(5)	5153.1	16^-	15^-	783.1(8)	2.4(4)	
1283.7	8^-	7^-	396.1(3)	14.2(12)	0.47(5)			15^-	835.2(8)	2.7(5)	
		6^-	789.6(4)	33.2(15)	1.00(9)			14^-	1083.1(9)	3.8(7)	
1498.2	8^-	8^-	217.7(5)	2.5(9)		5441.8	17^-	16^-	288.7(4)	6.0(15)	0.54(10)
		7^-	610.5(5)	6.3(9)	0.51(10)			16^-	664.6(7)	5.2(9)	0.48(9)
1710.5	9^-	8^-	427.1(5)	10(3)	0.48(5) [a]			15^-	1071.2(8)	18.6(27)	1.04(11)
		7^-	822.9(3)	23.2(14)	1.10(11)			15^-	1124.5(8)	13.5(16)	1.13(11)
		8^+	1436.3(8)	6.4(7)		5504.3	17^-	16^-	727(2)	1.8(4)	
2026.1	10^-	9^-	315.7(3)	15.0(5)	0.47(5)			15^-	1133.9(8)	13.4(15)	1.04(9)
		8^-	742.2(4)	35(8)	0.95(8)			15^-	1186.5(8)	11.4(14)	0.95(9)
		10^+	892.4(6)	3.3(4)	0.98(10)	5605.2	17^-	15^-	1287.6(10)	5.0(10)	0.88(11)
2209.4	(10^-)	8^-	711.2(9)	4.7(8)		6035.1	18^-	17^-	594(2)	2.1(4)	
2454.5	11^-	10^-	428.2(6)	10(3)	0.48(5) [a]			16^-	1258.2(8)	23.5(20)	0.91(9)
		9^-	744.1(7)	15(4)	0.92(8)	6479.2	19^-	18^-	(444)		
		10^+	1320.8(7)	9(3)				17^-	1037.4(8)	26.7(22)	1.11(14)
2599.0	11^-	10^-	573.0(5)	6.8(10)	0.57(9)	6807.7	19^-	17^-	1303.4(9)	20.6(20)	1.01(9)
2779.3	12^-	11^-	324.6(3)	22.1(15)	0.49(13)	6972.3	(19^-)	17^-	1367.1(10)	5.9(12)	
		10^-	753.2(5)	33.5(25)	1.02(13)	7460.3	20^-	18^-	1425.2(9)	21.9(20)	1.06(10)
		11^+	1178.5(6)	8.3(10)		7819.2	21^-	19^-	1340.0(9)	15.8(18)	1.04(15)
3065.2	(12^-)	(10^-)	855.8(10)	4.1(10)		8214.1	21^-	19^-	1406.4(9)	20.3(20)	0.98(9)
3302.0	13^-	12^-	522.8(4)	19.8(15)	0.54(10)	8428	(21^-)	(19^-)	1456(2)	1.8(5)	
		11^-	847.3(5)	6.8(10)		9064.4	22^-	20^-	1604.1(10)	14.2(15)	1.14(12)
3377.4	13^-	12^-	597.9(7)	9.7(12)	0.62(9)	9649	(23^-)	21^-	1830(3)	5.5(10)	
		11^-	778.7(7)	13.0(13)	1.04(21)	9728.5	23^-	21^-	1514.4(10)	15.6(16)	1.11(15)
		11^-	922.8(8)	14.7(14)	1.10(17)	10866.1	24^-	22^-	1801.7(12)	9.6(12)	0.91(10)
3687.1	14^-	13^-	385.3(4)	16.7(15)	0.52(10)	11456.8	25^-	23^-	1728.3(11)	11.2(13)	0.99(13)
		12^-	907.7(5)	46.5(20)	1.06(8)	12885	(26^-)	24^-	2019(3)	2.8(7)	
4069.9	14^-	13^-	767.6(4)	6.8(9)		13416.4	(27^-)	25^-	1959.6(14)	8.3(13)	
4317.6	15^-	14^-	630.5(5)	10.8(20)	0.49(6)	15094	(28^-)	(26^-)	2209(3)	<2	
		13^-	1015.6(9)	20(4)	0.91(7)	15661	(29^-)	(27^-)	2245(3)	4(1)	
4370.5	15^-	14^-	300.3(4)	5(1)	0.62(17)	18057	(31^-)	(29^-)	2396(3)	<2	
		13^-	993.1(7)	22.4(25)	0.92(8)	(20786)	(33^-)	(31^-)	(2729)		
4776.9	16^-	15^-	459.1(5)	6.2(7)	0.64(9)						

[a]Combined DCO ratio of the doublet.

scribed in Sec. II were performed at FSU. One possibility considered was that a low-energy γ ray connects the lowest 6^+ state in Fig. 1 with a 5^+ state just below it. Even after taking into account internal conversion, such a decay should be clearly visible because all of the ^{86}Nb γ-decay strength should proceed through it. No candidates were observed down to the lower limit of 12 keV. This makes the doublet hypothesis much less likely, although a smaller energy separation is still possible. The second follow-up experiment, a γ-γ coincidence measurement of the β decay of ^{86}Nb [25], shows a considerably extended β-decay scheme consistent with a spin and parity assignment of 6^+ for the ground state of ^{86}Nb.

B. Positive-parity states

The decay scheme of Fig. 1 is naturally divided into two approximately equal and almost independent halves. Most of the states on the left half are connected to the positive-parity ground state through transitions with DCO ratios near unity and presumably $E2$ character. Moreover, bands (3) and (4) share all the characteristics (such as generally yrast nature, reversal of signature splitting, and alternating $M1$ strengths) of the yrast positive-parity bands in other odd-odd nuclei. The decay scheme strongly suggests that almost all the states on the left side have positive parity and related configura-

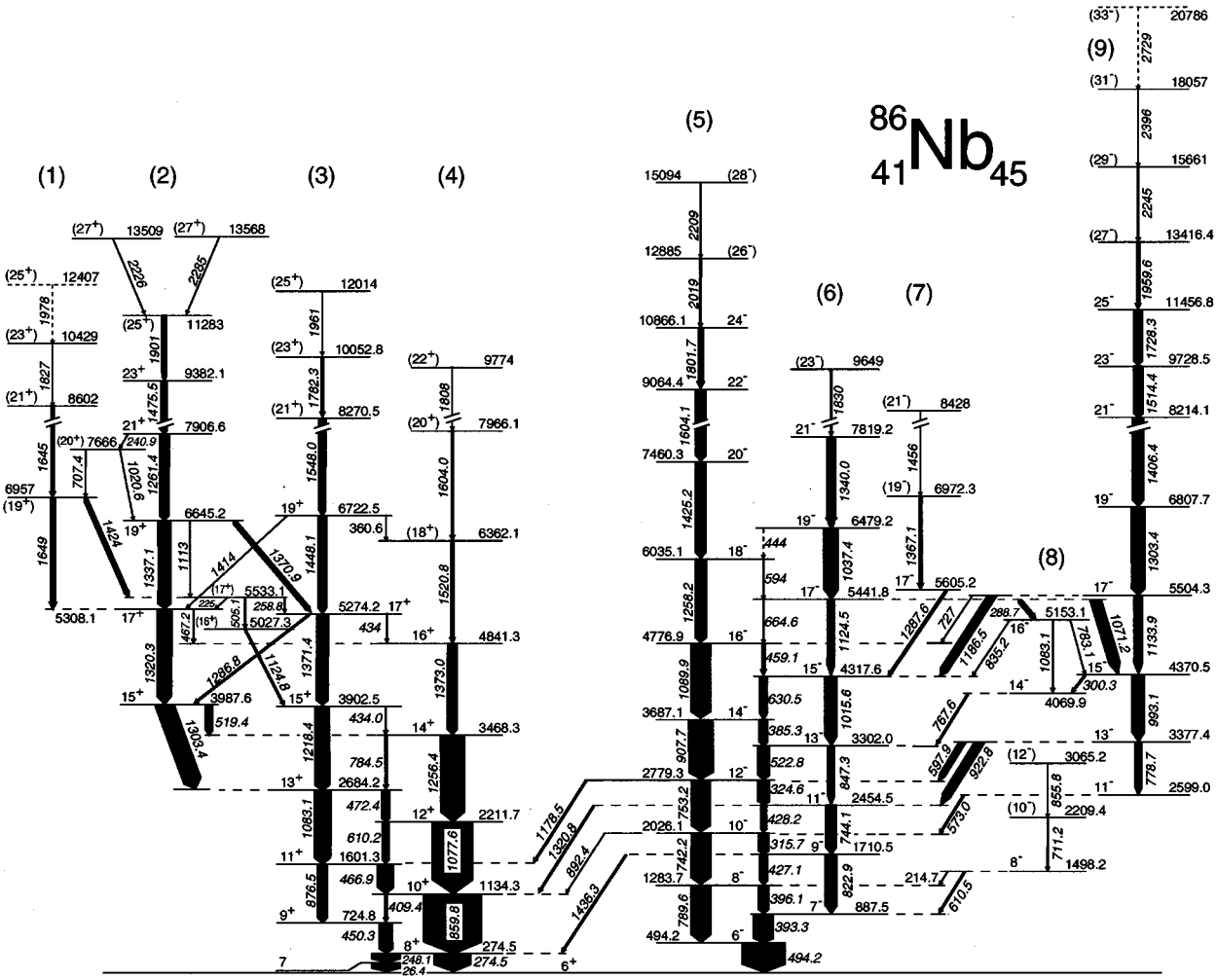

FIG. 1. The level scheme of ^{86}Nb as deduced from the present work. The question of whether the lowest state shown is the ground state is discussed in the text. Note that the vertical scale is reduced by a factor of 2 above an excitation energy of 8000 keV. The arbitrary numbers above the decay sequences are intended only to facilitate the discussion.

tions. An example of the particle-γ-γ-γ coincidence spectra of transitions among these states is shown in Fig. 2.

The lower parts of bands (3) and (4) correspond to one of the decay sequences reported in Ref. [17]. The 26.4 keV transition was well below the energy thresholds in the GAMMASPHERE experiment, although it was seen in the LEPS in the FSU experiment in weak coincidence with the 248.1 keV line. The weak coincidences suggest a long lifetime for the 26.4 keV state, perhaps on the order of a microsecond or longer. For this reason the order of the 26.4 and 248.1 keV transitions has been reversed relative to that shown in Ref. [17]. Although coincidences between lines at 248 and 782 keV, which suggested the ordering given in Ref. [17], were seen in the present work, no additional coincidences could be found in spite of much higher statistics. It is possible that a different 248 keV line is involved in the coincidences with the 782 keV line. For the level ordering shown in Fig. 1, transition strength arguments suggest that the 26.4 keV $I=7$ state may not have the same structure as the other states in bands (3) and (4) and could have negative parity. A search was made for transitions from other negative-parity states to the 26.4 keV level, but none were found. In summary, the level ordering shown is the most likely in view of the available evidence, but the question is not yet fully resolved.

The placements of the 1256.4-1261.4 keV doublet and the 1370.9-1371.4-1373.0 keV triplet are clear, although their exact energies, relative intensities, and DCO ratios are harder to determine. There is evidence for a second 434 keV decay between the 17^+ and 16^+ levels, but the gates which could clearly separate it are part of the unresolved triplet. The 1645-1649 keV doublet in band (1) is also unresolved and leads to uncertainties in determining the energies, intensities, and DCO ratios of those lines. Several weak, but clear, low-energy lines show the presence of three ''extra'' levels at 5027.3, 5533.1, and 7666 keV.

Another decay sequence begins with the 1303.4 keV line and several decays between this band (2) and band (3) show considerable mixing between them. No evidence was seen for other corresponding decays, such as from the 5308.1 keV level to the 3902.5 keV state or from the 21^+ states to the opposite 19^+ ones. The 2226 and 2285 keV lines are clearly in coincidence with other transitions in this sequence, as can be seen from Fig. 2. Within the somewhat limited statistics at the top of the band they do not appear to be in coincidence with each other. The grouping of states within each band is clear from the strongest $E2$ branches, except for the forking

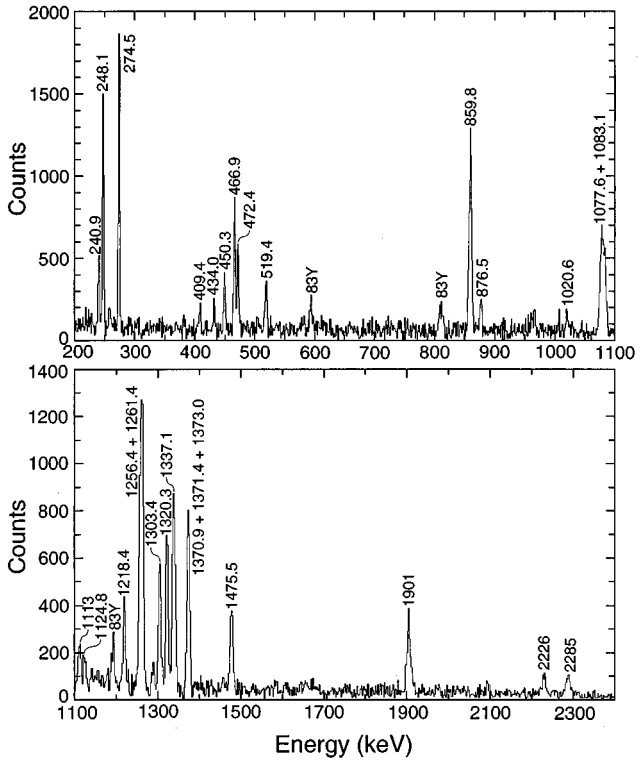

FIG. 2. The spectrum of γ rays in coincidence with three protons and no α particles and two other γ rays. One of the γ gates was the 1475.5 or 1901 keV line in band (2) and the other γ gate was the 248.1, 274.5, 450.3, 466.9, 472.4, 859.8, 1077.6, 1083.1, 1218.4, 1256.4, 1261.4, 1303.4, 1320.3, 1337.1, 1370.9, 1371.4, 1373.0, 1475.5, or 1548.0 line.

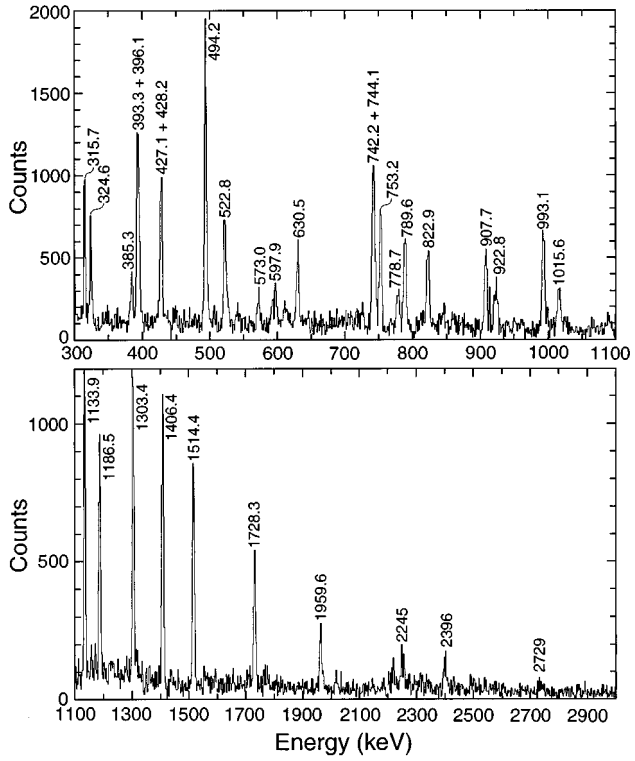

FIG. 3. The spectrum of γ rays in coincidence with two γ gates, one on the 315.7, 324.6, 393.3, 396.1, 427.1, 428.2, 494.2, or 789.6 line and another on the 1303.4, 1406.4, 1514.4, or 1728.3 keV line in band (9). Note that the vertical scale increases by a factor of 2 at 2200 keV.

which occurs at the 2684.2 keV state. The placement shown keeps band (3) as the yrast one up to about 6.6 MeV, has the most $M1$ branches between signature partners and gives the most uniform signature splitting curve.

The DCO ratios in Table I cluster around the expected values of about 0.5 and 1.0 for predominantly $M1$ and $E2$ transitions, respectively, and are consistent with the spins shown in the level scheme. Parentheses are used for the spins of states which could not be determined from the DCO ratios.

C. Negative-parity states

The states on the right half of the level scheme in Fig. 1 form a decay group almost completely separate from that of the positive-parity levels. Both from systematic and theoretical grounds these states are expected to have negative parity. Their structures typically involve at least one $g_{9/2}$ and one (fp) quasiparticle. An example of the γ-γ-γ coincidence relations among these transitions is shown in Fig. 3.

The lower parts of bands (5) and (6) generally correspond to group (A) in Ref. [17] although the 324.6 and 753.2 keV lines have now been placed somewhat higher in the decay scheme. The placement of the two unresolved doublets at 427.1-428.2 and 742.2-744.1 keV is clear, although their exact energies, intensities, and DCO ratios are more difficult to determine. No difference could be measured between the energies of the 1303.4 keV $15^+ \rightarrow 13^+$ and $19^- \rightarrow 17^-$ transitions, but their coincidence relations are quite distinct. Because of interconnecting transitions, the grouping of levels into bands (6) and (9) is not unique. The assignments shown in Fig. 1 provide that largest number of $\Delta I = 1$ decays between bands (5) and (6) and provide the most regular signature splitting pattern.

Many of the negative-parity lines, but not those lowest in the level scheme, were seen in the matrix gated by low-lying positive-parity transitions. Four connecting transitions were found between the otherwise separate positive- and negative-parity decay sequences. The energy relations involving the connecting transitions clearly show that the 494.2 keV decay leads to the same 6^+ level as do the 248.1 and 274.5 keV lines on the positive-parity side.

The DCO ratios of the 494.2 and 892.4 keV lines are consistent with either stretched $\Delta I = 2$ or $I \rightarrow I$ decay. The former possibility is extremely unlikely. $E2$ decay for these lines would imply that all of the states observed in the experiment have the same parity, in contradiction to all other nuclei in this region. $M2$ decay is also extremely unlikely since a number of much faster competing $E1$ decays are possible for these levels, but none have been observed. Another strong argument against $\Delta I = 2$ decay is that it would make the states on the right yrast while the strongest decay intensities are seen on the left side of the level scheme. The other possibility of $I \rightarrow I$ $E1$ decay fits all the observed systematics. The $M1$ possibility would also mean that no negative-parity states were seen in the experiment. The spin changes are generally well determined by the DCO ratios except for the weakest lines. Spins which could not be

clearly determined from the DCO ratios are shown in parentheses.

IV. DISCUSSION

A. Positive-parity yrast band

Decay sequences (3) and (4) are yrast up to 6 MeV. The regular increase in energy differences and other similarities with established rotational bands in nearby nuclei suggest a rotational nature, even though ^{86}Nb with 45 neutrons is expected [32] to be only moderately deformed. The rotational hypothesis can be tested by comparing the moments of inertia inferred from the experimental energies and spins with those of the yrast bands of nearby odd-odd nuclei. The kinematic moments of inertia $J^{(1)}$ for bands (3) and (4) fall from high values at low spins and then level off to about the rigid-body value $[(20-25)\hbar^2/\mathrm{MeV}]$ above a rotational frequency of $\hbar\omega \approx 0.4$ MeV, as shown in Fig. 4. This behavior is quite similar to that in nearby odd-odd nuclei, both those shown in Fig. 4 (^{84}Nb [17], ^{84}Y [10], and ^{82}Y [6–9]) and other lighter ones [12,33]. The relatively constant values of $J^{(1)}$ for $\hbar\omega > 0.4$ MeV strongly suggest a collective rotational interpretation for states above 9^+. Gentle rises in $J^{(1)}$ and modest peaks in the dynamic moments of inertia $J^{(2)}$ shown in Fig. 5 around $\hbar\omega \approx 0.7$ MeV indicate a qp alignment for both bands (3) and (4). Similar alignments can be seen in ^{82,84}Y, although the critical frequency varies somewhat.

Bands (3) and (4) appear to be signature partners connected by a number of $\Delta I = 1$ transitions. The behavior of the signature splitting can best be observed by graphing the normalized energy differences between states as a function of spin, as in Fig. 6. The alternating pattern indicates signature splitting which increases with spin in ^{86}Nb. The pattern reverses, however, below the 10^+ state. A rather similar behavior can also be seen for ^{84}Y [10] and ^{82}Y [6–9] in Fig. 6. In fact this pattern has been seen in the yrast bands of all odd-odd f-p-g shell nuclei for which sufficient information exists [12]. Above spin $10\hbar$ the phase of the alternations shows that the odd-spin states ($\alpha = 1$) are relatively lower in energy than the even-spin ones ($\alpha = 0$) and are thus favored. This agrees with the theoretical expectation that odd-spin states should be favored for rotational bands built on the $\pi g_{9/2} \otimes \nu g_{9/2}$ configuration, which provides the highest spin possible for two quasiparticles in the f-p-g shell.

A rather similar phase reversal in signature splitting was predicted near the 9^+ state in ^{76}Br from a 2-qp-plus-rotor calculation [13]. Recent 2-qp-plus-triaxial-rotor calculations [6] also show a change in the signature splitting at about the 9^+ state in ^{82}Y. In these calculations the change in signature splitting represents the onset of collective rotation above the maximum spin available for two unlike $g_{9/2}$ qp's, namely, $9\hbar$. At low spins the increase in spin up the band comes mainly from recoupling of the two qp's, while collective rotation dominates above the transition. This single-particle to collective transition has been mapped out by measuring the $E2$ transition strengths in ^{82}Y [34], which increase rather smoothly in the spin range of $(6-10)\hbar$. Because of the observed similarities among the yrast bands of odd-odd f-p-g shell nuclei, similar conclusions probably apply to the other cases, including ^{86}Nb. The change in the behavior of $J^{(1)}$ at about the same frequency ($\hbar\omega \approx 0.4$ MeV) is further evidence for this transformation in structure.

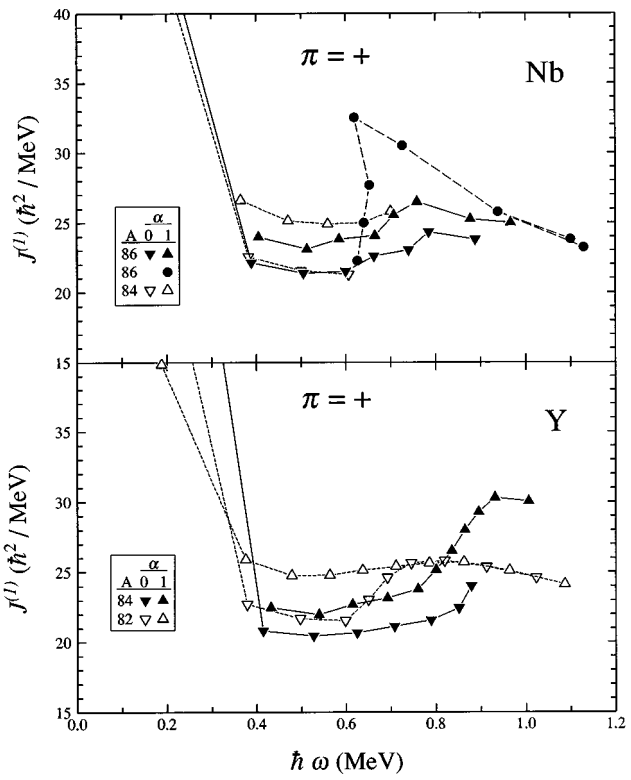

FIG. 4. Kinematic moments of inertia $J^{(1)}$ as a function of rotational frequency $\hbar\omega$ for positive-parity bands in odd-odd ^{86}Nb, ^{84}Nb [17], ^{84}Y [10], and ^{82}Y [6–9]. The ^{84}Nb graphs are based on a value of 8 for the variable J in Fig. 5 of Ref. [17] suggested by systematics. In the upper panel the solid circles, up-pointing triangles, and down-pointing triangles correspond to bands (2), (3), and (4) in Fig. 1, respectively. The two highest-frequency points represent the two parallel states at the top of band (2).

Another aspect of signature splitting involves the $B(M1)$ strengths of transitions between the signature partners [35]. The variations in the $M1$ strengths can be estimated from the branching ratios of the $\Delta I = 1$ and $\Delta I = 2$ intraband transitions. The following analysis has assumed that $M1$ transitions dominate the $\Delta I = 1$ decays, as is indicated by the measured DCO ratios. The $B(M1)$ to $B(E2)$ ratios implied by the measured branching ratios are shown in Fig. 7 and compared with those in ^{84}Y [10] and ^{82}Y [6,9]. Large alternations, with amplitudes of roughly an order of magnitude, can be seen in $B(M1)/B(E2)$ for all these nuclei. In fact, similar alternations occur in the yrast bands of all the lighter odd-odd f-p-g shell nuclei for which adequate information is available [12]. The amplitude of the alternations varies from case to case, but they always occur with the same phase.

Since the intraband $B(E2)$ strengths usually vary smoothly with spin, the alternations in Fig. 7 can be attributed to alternations with even and odd spin in the $B(M1)$ values. This has been proved in cases such as ^{82}Y [6,9,34] where the lifetimes have been measured. The 2-qp-plus-triaxial-rotor calculations [6] were able to qualitatively reproduce the $B(M1)$ alternations in ^{82}Y. In this

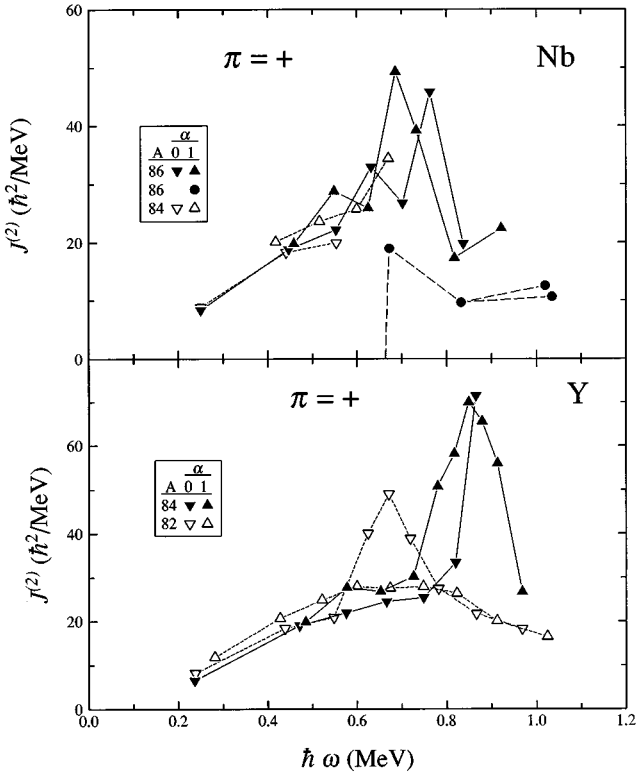

FIG. 5. Graphs similar to those in Fig. 4 for the dynamic moments of inertia $J^{(2)}$.

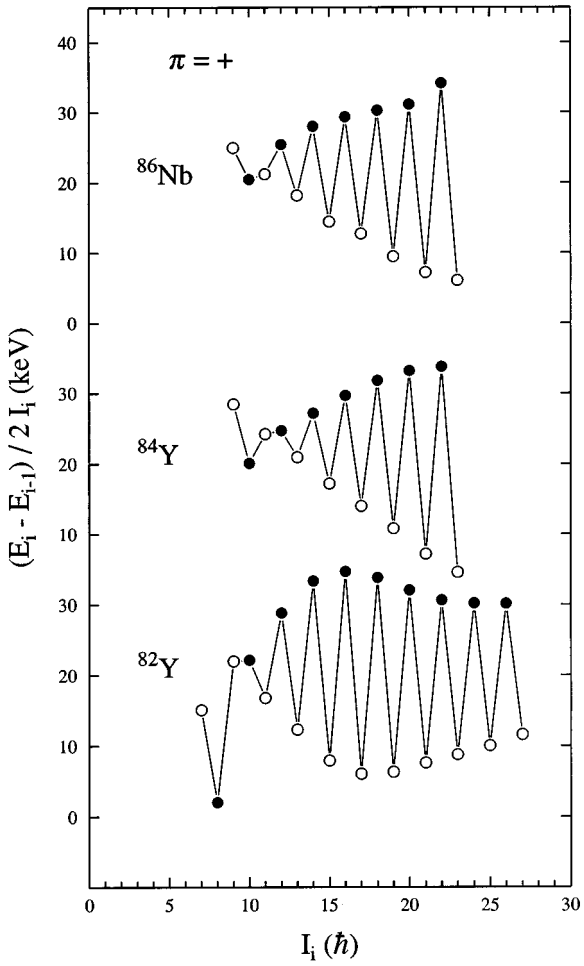

FIG. 6. Normalized energy differences $(E_i - E_{i-1})/2I_i$ between adjacent states in the yrast bands of ^{86}Nb, ^{84}Y [10], and ^{82}Y [6–9] as a function of the spin of the upper state I_i. For clarity, points with even (odd) I_i are shown with closed (open) circles.

model $M1$ transitions from an odd-spin state to the lower even-spin one are strong because they involve only a change in the qp-core coupling, while those from even to odd spin states are much weaker because they involve changes of the core rotational states. The contributions to the $M1$ transition rates from the odd neutron and odd proton alternate with the same phase, although which contribution dominates depends on the triaxiality parameter γ. This may explain why all the observed oscillations have the same phase. The alternations in energy splittings and $M1$ strengths shown in Figs. 6 and 7 are rather similar, but a careful comparison shows that the $M1$ alternations do not exhibit the phase reversal at low spins seen in the energy splittings.

B. Other positive-parity structures

A third decay sequence [(2) in Fig. 1] starts at the 3987.6 keV level and becomes yrast at the 6645.2 keV state. Since it appears at about the frequency of the band crossing in bands (3) and (4) and exhibits significant mixing with these bands in the spin range of $15^+ - 19^+$, it is probably also based on a 4 qp structure. The moment of inertia of band (2) starts with a sharp rise at $\hbar\omega \approx 0.6$ MeV in Fig. 4 and slowly drops back to the rigid-body value.

A clear signature partner has not been observed for band (2). The 5027.3 keV (16^+) and 7666 keV (20^+) states are possible candidates for energetically unfavored signature partners, but no candidate was seen for the 18^+ state and no $M1$ decays were observed between band (2) and the 5027.3 keV (16^+) state. Although firm spin assignments cannot be made for these weakly populated states, the 5533.1 keV level is unlikely to be the missing 18^+ state because it lies too low in energy, almost 1 MeV below the more strongly populated (18^+) level in band (4). It is more likely that the 5533.1 keV state represents a fully aligned nonrotational shell-model-like state [36]. The most likely spin for this state (17^+) is the maximum spin possible for six particles outside the filled $(N=3)$ shell coming from the configuration $\pi(g_{9/2})^1_{4.5} \otimes \nu(g_{9/2})^5_{12.5}$. (Note that this notation indicates particles relative to a filled $[N=3]$ shell, rather than quasiparticles relative to the ^{84}Zr vacuum as has been used for the earlier configuration descriptions.) The 5027.3 keV (16^+) level might be the related, not quite fully aligned $\pi(g_{9/2})^1_{4.5} \otimes \nu(g_{9/2})^5_{11.5}$ state.

At the expense of additional energy a maximum spin of 27^+ can be generated with two holes in the $[N=3]$ shell with the configuration $\pi[N=3]^{-2}_4 (g_{9/2})^3_{10.5} \otimes \nu(g_{9/2})^5_{12.5}$. There appears to be some change in the band structure at the (27^+) states. The calculations of Afanasjev and Ragnarsson have provided strong evidence for fully aligned shell-model-like states in the nearby nucleus ^{86}Zr [25].

The unresolved 1645-1649 keV doublet prevented firm spin determinations in band (1). However, it is unlikely to be the signature partner of band (2) because no states were seen below the 6957 keV level and even spins are unlikely for

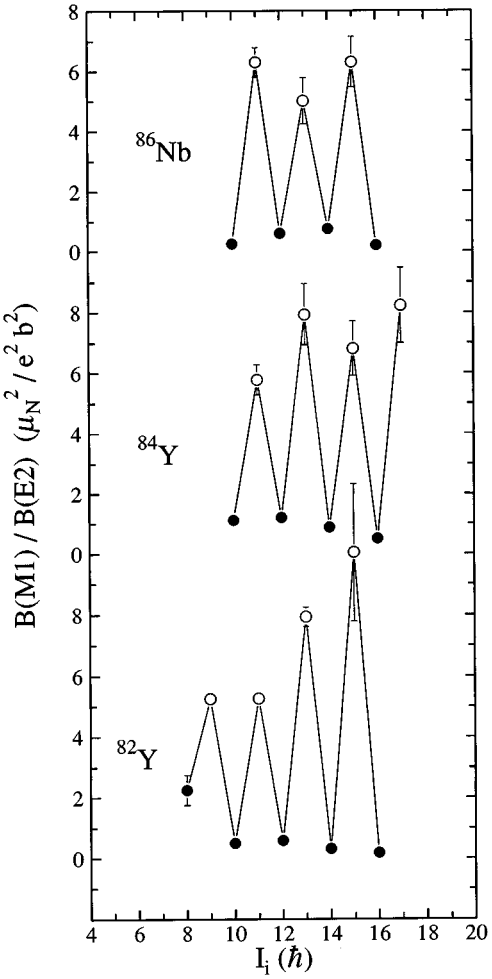

FIG. 7. Ratios of $M1$ to $E2$ strengths inferred from the branching ratios of $\Delta I=1$ and $\Delta I=2$ transitions in the positive-parity yrast bands of ^{86}Nb, ^{84}Y [10], and ^{82}Y [6,9]. For clarity, points with even (odd) I_i are shown with closed (open) circles.

band (1). The only possible even spin for the 6957 keV state would be (18^+) but this would imply that either the 240.9 or 707.4 keV transition has $\Delta I=2$. Such relatively low energy $E2$ decays would not be likely to compete with the available $M1$ and higher energy $E2$ decay modes.

C. Negative-parity bands (5) and (6)

The lowest negative-parity decay sequences, (5) and (6), do not show the increasing energies for $\Delta I=2$ transitions expected for good rotors below the 12^- state. This low-spin behavior may result from the transitional nature of ^{86}Nb. All the observed decays to the positive-parity bands occur in this low-spin region, indicating perhaps weaker intraband $E2$ transition strengths and/or more configuration mixing.

Above the 12^- state, the energy spacings do follow the characteristic rotational pattern. The kinematic moments of inertia $J^{(1)}$ inferred from bands (5) and (6) assuming a rotational interpretation are shown in Fig. 8. On this graph the initial rise in $J^{(1)}$ at $\hbar\omega\approx$ 0.35 MeV (corresponding to states below 12^-) looks like a qp alignment. The moment of inertia then gradually falls from the peak value of $30\hbar^2$/MeV toward the rigid body value of $(20–25)\hbar^2$/MeV. Another

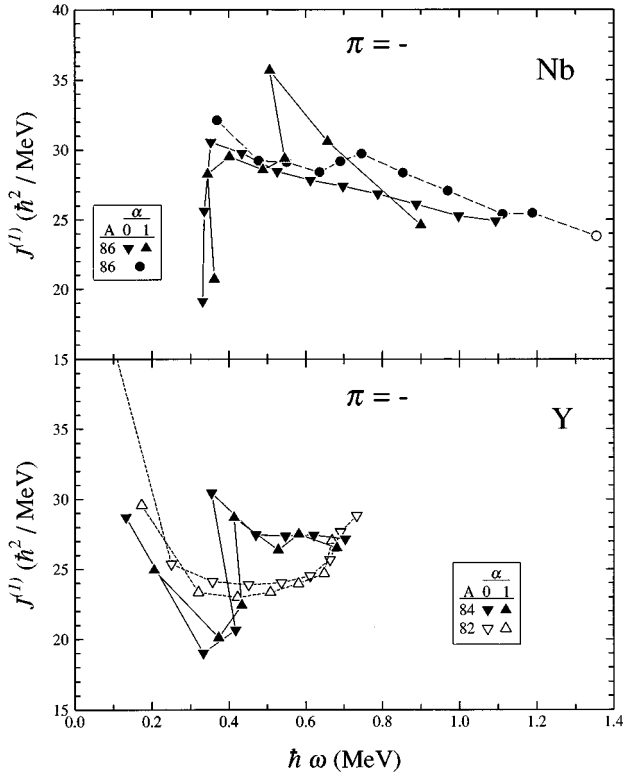

FIG. 8. Kinematic moments of inertia $J^{(1)}$ as a function of rotational frequency $\hbar\omega$ for negative-parity bands in odd-odd ^{86}Nb, ^{84}Y [10], and ^{82}Y [6–9]. In the upper panel the solid circles, up-pointing triangles, and down-pointing triangles correspond to bands (9), (6), and (5) in Fig. 1, respectively.

backbend occurs at $\hbar\omega\approx$ 0.5 MeV, but only in the $\alpha=1$ odd-spin band. Quite surprisingly the curve for the $\alpha=0$ even-spin band is very smooth in this region. The moments of inertia for the corresponding lowest negative-parity bands in ^{82}Y [6,7,9] and ^{84}Y [10] are also shown in Fig. 8 for comparison. The behavior of $J^{(1)}$ in ^{84}Y for $\hbar\omega>$ 0.3 MeV is quite similar to that for the isotone ^{86}Nb. Both rise quickly from about $20\hbar$/MeV to about $30\hbar^2$/MeV and then gradually fall. This comparison suggests that an extended qp alignment may be occurring in the spin range of 6^- – 12^- in ^{86}Nb.

Bands (5) and (6) appear to be signature partners with many connecting $\Delta I=1$ transitions. Their signature splittings are compared with those of comparable bands in two odd-odd Y isotopes in Fig. 9. The graph for ^{86}Nb appears divided into three regions. The first three points show wide energy spacings, but little signature splitting. This is the low-spin region where transition energies change little and the kinematic moments of inertia rise vertically. The middle region from $10\hbar$ to $18\hbar$ shows a consistent and moderate signature splitting with even spins or the $\alpha=0$ signature energetically favored. The magnitude of the signature splitting is about a factor of 2 less than in the positive-parity yrast band and has the opposite phase. However, the signature splittings have the same phase in the negative-parity bands of all three nuclei, at least in the middle spin region.

In the third region above $18\hbar$, the phase of the signature splitting in ^{86}Nb reverses and the magnitude increases by about a factor of 2. This transition from region (2) to (3)

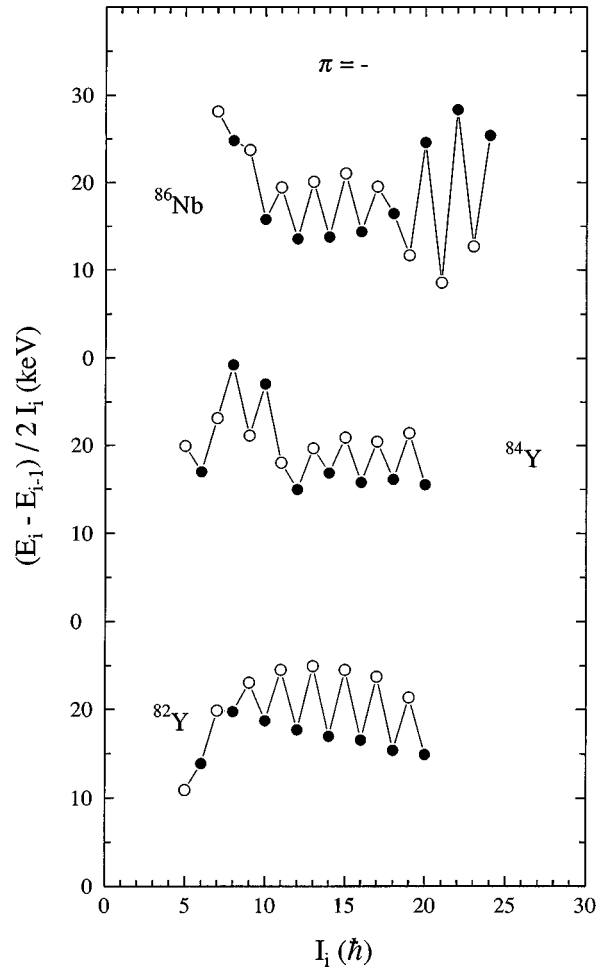

FIG. 9. Normalized energy differences $(E_i - E_{i-1})/2I_i$ between adjacent states in the lowest negative-parity bands of ^{86}Nb, ^{84}Y [10], and ^{82}Y [6,7,9] as a function of the spin of the upper state I_i. For clarity, points with even (odd) I_i are shown with closed (open) circles.

corresponds to the sharp backbend observed in the signature $\alpha = 1$ band and presumably to a transition from a 2 qp to a 4 qp structure. A reversal in the phase of the signature splitting is also observed in ^{84}Y, but it occurs at a lower spin and the phase of the splitting above the reversal corresponds to the middle, rather than upper, region of signature splitting in ^{86}Nb.

D. Negative-parity bands (7), (8), and (9)

Somewhat in analogy with band (2) on the positive-parity side, band (9) starts at about 2.6 MeV and eventually carries much of the negative-parity decay strength. The trend from the energies of lower states and the fact that band (9) has been observed to the highest spins [(31^-) and tentatively (33^-)] suggest that it becomes yrast above the 23^- level, the last state known in band (6). Figure 8 shows that band (9) appears just above the upbend in bands (5) and (6) and its kinematic moment of inertia parallels that of band (5). There is a small peak in $J^{(1)}$ at $\hbar\omega \approx 0.75$ MeV which does not occur in band (5), but it is much smaller than the backbend seen only in band (6). Strong decay intensities between band

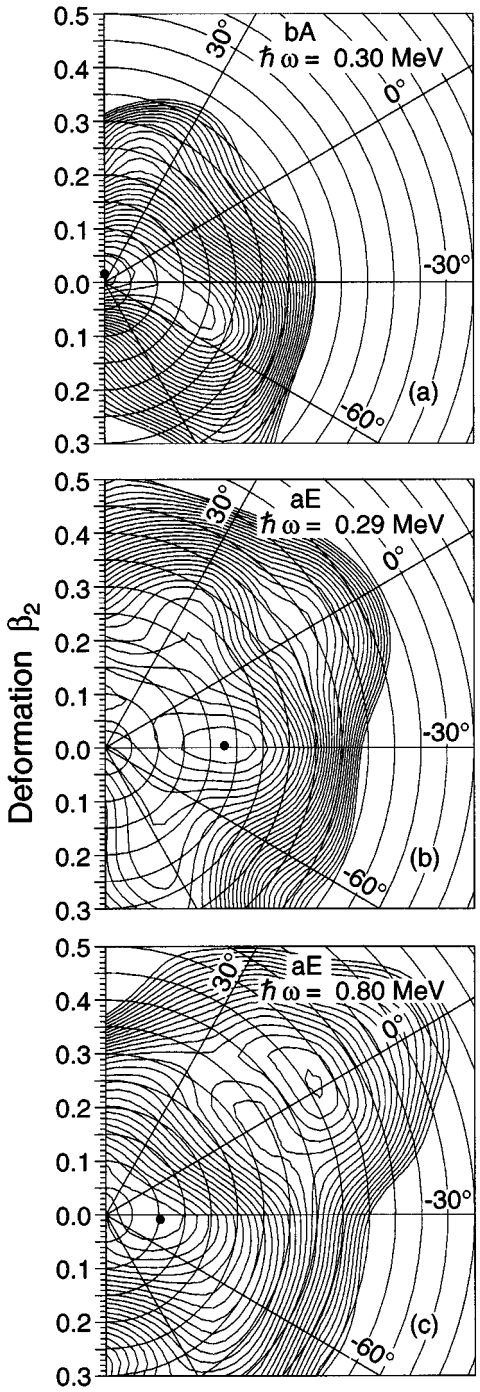

FIG. 10. Calculated total Routhian surfaces for the indicated configurations (convention of Ref. [38]) and rotational frequencies for ^{86}Nb. The spacing between contour lines is 150 keV for the middle and top panels and 250 keV for the bottom panel.

(9) and bands (5) and (6) indicate considerable mixing between the structures in the range from the 11^- to the 17^- states.

The states shown under the label (8) in Fig. 1 form two decay sequences. The 4069.9 keV 14^- and 5153.1 keV 16^- states may be signature partners for band (9), since two connecting $M1$ transitions were observed. If so, they indicate much more signature splitting than in bands (5) and (6), and their position as rather energetically unfavored may explain why they are so weakly populated. The positions of the three

lower states at 1498.2, 2209.4, and 3065.2 keV suggest that they might also be signature partners for band (9) and a continuation of the upper decay structure. However, no convincing evidence was found for decays between the 4069.9 keV 14^- and 3065.2 keV (12^-) levels for $M1$ transitions between the three lower even-spin states and band (9).

A third odd-spin band (7) begins with the 5605.2 keV 17^- state, but it is populated rather weakly and only a few members were seen.

E. Hartree-Fock-Bogolyubov cranking calculations

Hartree-Fock-Bogolyubov cranking calculations [37] were performed for configurations in ^{86}Nb using a Woods-Saxon potential and a short-range monopole pairing force. Representative total Routhian surfaces (TRS's) in the (β_2,γ) plane are shown in Fig. 10. At each grid point, the Routhian was minimized with respect to the hexadecapole deformation β_4. The label ''bA'' (see Ref. [38]) represents the lowest proton and neutron configuration with overall positive parity and odd spin, while ''aE'' is the lowest 2 qp configuration with overall negative parity and odd spin.

Although the positive-parity TRS (labeled ''bA'') shows considerable β softness, a moderately deformed, almost oblate shape of $\beta_2\approx 0.2$ and $\gamma\approx -50°$ is predicted for band (3). A similar shape is predicted for band (4) from the TRS for the ''aA'' configuration. At higher rotational frequencies an additional highly deformed prolate shape with $\beta_2\approx 0.45$ is predicted, similar to that shown at the bottom of Fig. 10. This shape may correspond to band (2) which becomes yrast at higher spins or, perhaps, to some more weakly populated band, not yet observed.

Triaxial shapes with moderate deformation ($\beta_2\approx 0.23$ and $\gamma\approx -30°$), such as that shown in the middle panel of Fig. 10, are predicted for the negative-parity bands at low rotational frequencies. Presumably, these represent bands (5) and (6). At higher rotational frequencies, additional more strongly deformed prolate shapes are predicted with $\beta_2\approx 0.33$ and 0.46. Band (9), which was observed to the highest spins, may correspond to one of these more strongly deformed shapes.

V. SUMMARY

The high-spin structure of ^{86}Nb was investigated using the early implementation of GAMMASPHERE and the MICROBALL following population in the ^{58}Ni(^{32}S,3pn)^{86}Nb reaction with a 135 MeV beam from the 88-Inch Cyclotron at Lawrence Berkeley National Laboratory. Follow-up experiments were performed at Florida State University to confirm the spin-parity assignment of 6^+ for the ground state of ^{86}Nb. The two sets of previously known decay sequences were generally confirmed and greatly extended. Decays between these bands established their relative positions for the first time. A number of new bands were discovered. Some of them compete with the lower-lying bands and eventually become yrast.

Bands (3) and (4), built on the 6^+ ground state, are yrast up to 6 MeV and show many similarities with the yrast bands of other odd-odd f-p-g shell nuclei: Their moments of inertia fall from high values down to the rigid-body values at $\hbar\omega\approx$ 0.4 MeV and then level off. Their signature splittings reverse phase at about the 10^+ level. Above this the signature splittings are rather large and show that odd-spin states are energetically favored. The $B(M1)/B(E2)$ strengths oscillate by as much as an order of magnitude, with those from odd- to even-spin states much stronger than vice versa. All of these characteristics are consistent with an intrinsic $\pi g_{9/2}\otimes\nu g_{9/2}$ structure in which angular momentum comes first predominantly from increasing qp alignment and then from collective rotation at higher spins.

Significant differences are also seen compared to the lighter, generally more deformed, odd-odd nuclei. A new positive-parity band appears at $E_x\approx 4$ MeV, mixes strongly with the yrast band in the region of its backbend, and then becomes yrast itself. Some additional weakly populated states are also seen which may be fully and nearly fully aligned shell-model-like states with configurations such as $\pi(g_{9/2})^1_{4.5}\otimes\nu(g_{9/2})^5_{12.5}$ relative to a filled $[N=3]$ core.

The lowest negative-parity bands start with a sharp upbend in the moment of inertia at $\hbar\omega\approx$ 0.35 MeV analogous to the upbend in the isotone ^{84}Y. At higher frequencies a sharp backbend occurs only in the $\alpha=1$ signature. A new $\alpha=1$ band starts above the upbend with a moment of inertia which roughly parallels that of the $\alpha=0$ band. The new band apparently becomes yrast at about 10 MeV and could be observed up to a tentative (33^-) level. This new band also mixes strongly with the lowest bands in a limited spin range.

ACKNOWLEDGMENTS

This work was supported in part by the National Science Foundation under Grant No. PHY-9210082 (FSU) and in part by the Department of Energy under Contract Nos. DE-AC05-76OR00033 (UNISOR), DE-AC05-96OR22464 (ORNL), DE-FG05-88ER40406 (WU), and DE-AC03-76SF00098 (LBNL).

[1] S.G. Buccino, F.E. Durham, J.W. Holcomb, T.D. Johnson, P.D. Cottle, and S.L. Tabor, Phys. Rev. C **41**, 2056 (1990).

[2] D.F. Winchell, J.X. Saladin, M.S. Kaplan, and H. Takai, Phys. Rev. C **41**, 1264 (1990).

[3] J.W. Holcomb, T.D. Johnson, P.C. Womble, P.D. Cottle, S.L. Tabor, F.E. Durham, and S.G. Buccino, Phys. Rev. C **43**, 470 (1991).

[4] J. Döring, G. Winter, L. Funke, B. Cederwall, F. Lidén, A. Johnson, A. Atac, J. Nyberg, G. Sletten, and M. Sugawara, Phys. Rev. C **46**, R2127 (1992).

[5] A. Harder, M.K. Kabadiyski, K.P. Lieb, D. Rudolph, C.J. Gross, R.A. Cunningham, F. Hannachi, J. Simpson, D.D. Warner, H.A. Roth, Ö. Seppstedt, W. Gelletly, and B.J. Varley, Phys. Rev. C **51**, 2932 (1995).

[6] P.C. Womble, J. Döring, T. Glasmacher, J.W. Holcomb, G.D. Johns, T.D. Johnson, T.J. Petters, M.A. Riley, V.A. Wood,

S.L. Tabor, and P. Semmes, Phys. Rev. C **47**, 2546 (1993).
[7] J. Mukai, A. Odahara, H. Tomura, S. Suematsu, S. Mitarai, T. Kuroyanagi, D. Jerrestam, J. Nyberg, G. Sletten, A. Atac, S.E. Arnell, H.A. Roth, and Ö. Skeppstedt, Nucl. Phys. **A568**, 202 (1994).
[8] G. García-Bermúdez, H. Somacal, M.A. Cardona, A. Filevich, E. Achterberg, and L. Szybisz, Phys. Rev. C **51**, 1181 (1995).
[9] S.D. Paul, H.C. Jain, S. Chattopadhyay, M.L. Jhingan, and J.A. Sheikh, Phys. Rev. C **51**, 2959 (1995).
[10] S. Chattopadhyay, H.C. Jain, S.D. Paul, J.A. Sheikh, and M.L. Jhingan, Phys. Rev. C **49**, 116 (1994).
[11] R.A. Kaye, J. Döring, J.W. Holcomb, G.D. Johns, T.D. Johnson, M.A. Riley, G.N. Sylvan, P.C. Womble, V.A. Wood, S.L. Tabor, and J.X. Saladin, Phys. Rev. C **54**, 1038 (1996).
[12] S.L. Tabor, Heavy Ion Phys. **2**, 239 (1995).
[13] A.J. Kreiner and M.A.J. Mariscotti, Phys. Rev. Lett. **43**, 1150 (1979).
[14] K. Oxorn, S.K. Mark, J.E. Kitching, and S.S.M. Wong, Z. Phys. A **321**, 485 (1985).
[15] R. Schubart, A. Jungclaus, A. Harder, M.K. Kabadiyski, K.P. Leib, D. Rudolph, M. Weiszflog, S. Albers, T. Burkardt, J. Eberth, M. Eschenauer, M. Luig, N. Nicolay, and H. Grawe, Nucl. Phys. **A591**, 515 (1995).
[16] D. Rudolph, M.K. Kabadiyski, K.P. Lieb, R. Schubart, M. Weiszflog, and H. Grawe, Phys. Scr. **T56**, 120 (1995).
[17] C.J. Gross, K.P. Lieb, D. Rudolph, M.A. Bentley, W. Gelletly, H.G. Price, J. Simpson, D.J. Blumenthal, P.J. Ennis, C.J. Lister, Ch. Winter, J.L. Durell, B.J. Varley, Ö. Skeppstedt, and S. Rastikerdar, Nucl. Phys. **A535**, 203 (1991).
[18] G. Korschinek, E. Nolte, H. Hick, K. Miyano, W. Kutschera, and H. Morinaga, Z. Phys. A **281**, 409 (1977).
[19] S. Della Negra, D. Jacquet, and Y. Le Beyec, Z. Phys. A **308**, 243 (1982).
[20] E.K. Warburton, C.J. Lister, J.W. Olness, P.E. Haustein, S.K. Saha, D.E. Alburger, J.A. Becker, R.A. Dewberry, and R.A. Naumann, Phys. Rev. C **31**, 1211 (1985).
[21] T. Shizuma, M. Kidera, E. Ideguchi, A. Odahara, H. Tomura, S. Suematsu, T. Kuroyanagi, Y. Gono, S. Mitarai, J. Mukai, T. Komatsubara, K. Furuno, and K. Heiguchi, Z. Phys. A **348**, 25 (1994).
[22] I.Y. Lee, Nucl. Phys. **A520**, 641c (1990).
[23] D.G. Sarantites, P.-F. Hua, M. Devlin, L.G. Sobotka, J. Elson, J.T. Hood, D.R. LaFosse, J.E. Sarantites, and M.R. Maier, Nucl. Instrum. Methods Phys. Res. A **381**, 418 (1996).
[24] S.L. Tabor, Nucl. Instrum. Methods Phys. Res. A **265**, 495 (1988).
[25] J. Döring *et al.* (unpublished).
[26] H.-W. Müller, Nucl. Data Sheets **56**, 551 (1989).
[27] J. Döring (private communication).
[28] D. Bucurescu, G. Constantinescu, D. Cutoiu, M. Ivaşcu, N.V. Zamfir, and A. Abdel Haliem, J. Phys. G **10**, 1189 (1984).
[29] C.J. Lister, J.W. Olness, E.K. Warburton, J.A. Becker, and S.D. Bloom, Phys. Rev. C **32**, 311 (1985).
[30] K. Oxorn and S.K. Mark, Z. Phys. A **316**, 97 (1984).
[31] C.A. Fields, F.W.N. De Boer, J.J. Kraushaar, R.A. Ristinen, L.E. Samuelson, and E. Sugarbaker, Nucl. Phys. **A363**, 311 (1981).
[32] S.L. Tabor, Phys. Rev. C **34**, 311 (1986).
[33] S.L. Tabor, Phys. Rev. C **45**, 242 (1992).
[34] G.D. Johns, K.A. Christian, R.A. Kaye, S.L. Tabor, G. García-Bermúdez, M.A. Cardonna, A. Filevich, H. Somacal, and L. Szybisz, Phys. Rev. C **53**, 1541 (1996).
[35] G.B. Hagemann and I. Hamamoto, Phys. Rev. C **40**, 2862 (1989).
[36] A.V. Afanasjev and I. Ragnarsson, Phys. Scr. **T56**, 220 (1995).
[37] W. Nazarewicz, J. Dudek, R. Bengtsson, T. Bengtsson, and I. Ragnarsson, Nucl. Phys. **A435**, 397 (1985).
[38] R. Wyss, F. Lidén, J. Nyberg, A. Johnson, D.J.G. Love, A.H. Nelson, D.W. Banes, J. Simpson, A. Kirwan, and R. Bengtsson, Nucl. Phys. **A503**, 244 (1989).